Infiltration and Inversion of Holographically Defined Polymer Photonic Crystal Templates by Atomic Layer Deposition**

By *Jeffrey S. King, Elton Graugnard, Olivia M. Roche, David N. Sharp, Jan Scrimgeour, Robert G. Denning, Andrew J. Turberfield*, and *Christopher J. Summers**

The demonstration of a practical technology for 3D optical microfabrication is a vital step in the development of photonic-crystal-based optical signal processing.[1] However, the extension of the optical methods that dominate integrated electronic circuit fabrication to three dimensions is a formidable materials-processing challenge: such a process must be capable not only of sub-micrometer pattern definition in three dimensions, but also of the transfer of this pattern into a homogeneous dielectric with an appropriately high refractive index. In a companion paper,[2] we show that two optical methods, holographic lithography[3] and direct two-photon laser writing,[4–6] can be combined to create a rapid and flexible method for the definition of photonic crystal device structures in photoresist. In this communication, we report a further essential step towards the creation of devices operating within a full photonic bandgap: we have used atomic layer deposition (ALD), itself an established semiconductor processing technique, to create high-index TiO_2 inverted replicas of holographically defined photonic crystals, followed by removal of the polymeric template by plasma etching.

A range of techniques for 3D optical lithography has been demonstrated. A 3D photonic crystal structure can be written by holographic lithography,[3] which makes use of a periodic interference pattern generated by a multiple-beam interferometer to expose a thick layer of photoresist. 3D microstructures, both periodic and aperiodic, can also be generated by point-by-point exposure of the resist by two-photon absorption at a laser focus.[4–7] Two-photon laser writing is a serial process; point-by-point fabrication of a 3D photonic crystal is necessarily slower than holographic lithography, which is capable of defining the entire periodic structure in a single laser pulse.[3] The two techniques are complementary: two-photon laser writing can be used to modify a holographic exposure.[8] We have shown that, by imaging the distribution of photochemical change induced by holographic exposure, it is possible to align a subsequent two-photon exposure with the 3D photonic crystal lattice to achieve the precise registration that is required of a device structure embedded in a 3D photonic crystal.[2] This hybrid technique is rapid and flexible, but the polymeric resists used for 3D microfabrication have refractive indices *n* in the range 1.4–1.6, which is too low for most device applications. Devices based on waveguides and microcavities embedded within a photonic crystal[1] are designed to operate at frequencies within a complete (omnidirectional) photonic bandgap in order to suppress radiative loss;[9] to create a complete photonic bandgap, even in an optimized air-dielectric structure, a refractive contrast of at least 1.9 is necessary.[10–12] This limitation may be overcome by using the polymeric structure as a template for infiltration to create a negative or (via a two-stage process) positive replica in a high-index dielectric. Integration of rapid and inexpensive optical fabrication with a compatible infiltration technique would constitute an important step toward the creation of a robust and scalable technology for nanofabrication of photonic devices.

The infiltration technique adopted must be capable of filling a multiply connected network of sub-micrometer channels to produce a dense and homogeneous network of transparent amorphous or nanocrystalline material, extending uniformly through a layer many unit cells deep. It must also be compatible with the low thermal decomposition temperature ($\sim 300\,°C$) of the epoxy resist used for holographic lithography.[2,3] Although chemical vapor deposition (CVD) has been used to back-fill silica opals with silicon, the high thermal decomposition temperature of the CVD precursors makes this process incompatible with most polymeric templates. For example, silane requires a substrate temperature of $550\,°C$,[13] while disilane deposition occurs at ca. $300\,°C$.[14] One solution to this problem is to adopt a double structural inversion. First, the polymer template is filled with SiO_2 at room temperature and atmospheric pressure using several cycles of exposure to $SiCl_4$ and water,[15] or by a sol–gel process.[16] Then, following removal of the template by oxidation, silicon can be grown by disilane CVD using the SiO_2 as a template.[14] Liquid-phase infiltration is also possible: opals have been filled with TiO_2

[*] Prof. C. J. Summers, Dr. J. S. King,[+] Dr. E. Graugnard
School of Materials Science and Engineering
Georgia Institute of Technology
Atlanta, GA 30332 (USA)
E-mail: chris.summers@mse.gatech.edu
O. M. Roche, Dr. D. N. Sharp, J. Scrimgeour, Prof. A. J. Turberfield
Department of Physics, University of Oxford
Oxford OX1 3PU (UK)
Prof. R. G. Denning
Inorganic Chemistry Laboratory, University of Oxford
Oxford OX1 3QR (UK)

[+] Present address: Department of Chemical Engineering, Stanford University, Stanford, CA 94305-5025, USA.

by sol–gel deposition of the anatase phase within the voids of the structure[17] or by assembling the opal in the presence of a concentrated dispersion of anatase nanoparticles.[18] In both cases, removal of the template by calcination leads to shrinkage of the TiO_2 infill and poor long-range structural order.

In order to develop a well-controlled infiltration technique for optically fabricated 3D microstructures, we have explored the potential of ALD,[19] a method that has been used successfully for the formation of single- and multicomponent inverse opals.[20–24] ALD utilizes sequential reactant pulses, separated by inert-gas purges, to force surface-limited reactions, thereby allowing the growth of dense, highly conformal films with submonolayer control. If precursor doses are sufficient to cause surface saturation, then conformal growth occurs and pores with extremely high aspect ratios can be uniformly infiltrated.[25] Amorphous TiO_2, the material that we have chosen, is deposited using alternating pulses of $TiCl_4$ and water vapor.[26] $TiCl_4$ reacts with surface hydroxyl groups to yield a layer in which titanium(IV) is covalently bound to the surface by oxygen but is terminated by Ti–Cl bonds. A subsequent pulse of water vapor hydrolyses these bonds to restore a hydroxyl-terminated surface. Initiation of a similar growth cycle on a polymer surface has been demonstrated.[27] Both stages are exothermic and proceed rapidly below 100 °C, a temperature that is compatible with the polymer template. ALD-deposited amorphous TiO_2 is dense and homogeneous, with $n > 2.3$ and low absorption down to UV wavelengths.[28] This route to a high-index structure is clearly simpler and more robust than the double-inversion techniques mentioned above and produces denser and more complete infiltration than sol–gel deposition.[20]

Resist layers 10 μm in thickness were holographically patterned to create photonic crystals with space group $R32$.[29] A unit cell of the rhombohedral lattice contains a prolate spheroid of developed resist with a long axis along the [111] direction. Each spheroid is connected by bridges to six of its twelve neighbors, three each in the planes above and below; the connectivity of this structure is the same as that of diamond. The spacing between (111) planes in the developed structure was measured by scanning electron microscopy (SEM) to be 615 nm and the distance between nearest neighbors within a (111) plane to be 490 nm. This measurement indicates that the developed template shrinks by a factor of 0.85 compared to the original interference pattern.

The developed, holographically patterned polymer templates were placed on quartz substrates in a custom, flow-style, hot-wall ALD reactor.[28] During deposition, the reactor temperature was maintained at 100 °C and the gas pressure at 0.2 ~ 0.5 Torr (1 Torr ~ 133 Pa).[20] The template was exposed to alternating 8 s pulses of $TiCl_4$ and water vapor separated by 20 s nitrogen purges. This deposition sequence resulted in highly conformal, homogeneous infiltration of the pores of the photonic crystal, with a growth rate of 0.51 Å per cycle. Conformal deposition in porous structures does not produce 100 % infiltration of the air voids: infiltration can only proceed as long as gas-flow pathways exist, and deposition is terminated by closure of pore channels at their narrowest points. Figure 1a shows an SEM image of the top surface of the polymer template before infiltration; this surface is closely aligned with a (111) plane. An arrow indicates the limiting aperture which determines the maximum deposition thickness that can
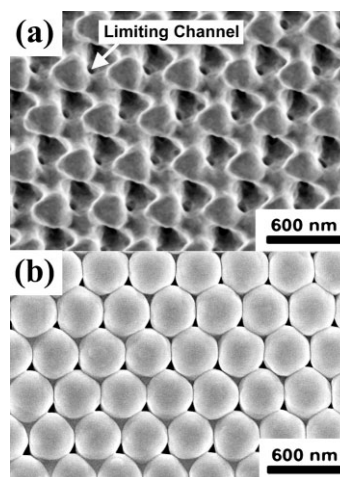
Figure 1. (111) surface of holographically generated epoxy template a) before infiltration and b) after ALD infiltration with 50 nm of TiO_2.

be achieved in the bulk of the structure; its diameter was estimated to be 100 nm. The number of applied ALD cycles was therefore limited to 980 cycles, corresponding to the maximum conformal infiltration thickness of 50 nm. Figure 1b shows the same surface after application of 980 ALD cycles: it is evident that a highly conformal film has been deposited on the polymeric template.

To maximize the refractive-index contrast in these composite structures, it was necessary to remove the polymer template after infiltration to create a photonic crystal consisting of interpenetrating lattices of TiO_2 and air. The top layer of TiO_2 was first removed by argon-ion milling to expose a section through the polymer template. Etching with an oxygen plasma for 1 h then successfully removed the template without damage. SEM images of the resulting structure are shown in Figure 2. These clearly show the successful formation of a uniform, high-quality TiO_2/air photonic crystal and complete removal of the polymer template. Figure 2a and b shows a (11$\bar{1}$) cleavage plane at two different magnifications, demonstrating uniform and homogeneous infiltration through the depth of the film. Figure 2b also shows that the surface of the holographic template was slightly misaligned (~5°) with the (111) planes, as previously reported.[3] Figure 2c and d shows a (111) surface of the structure. Comparison with Figure 1a shows that the TiO_2 photonic crystal is a near-exact inverse replica of the polymer template.

Figure 3 shows optical properties of the polymer template, the polymer/TiO_2 composite, and the TiO_2/air photonic crystal. A custom microreflectivity/microtransmission system allowed simultaneous measurement of both reflectivity and
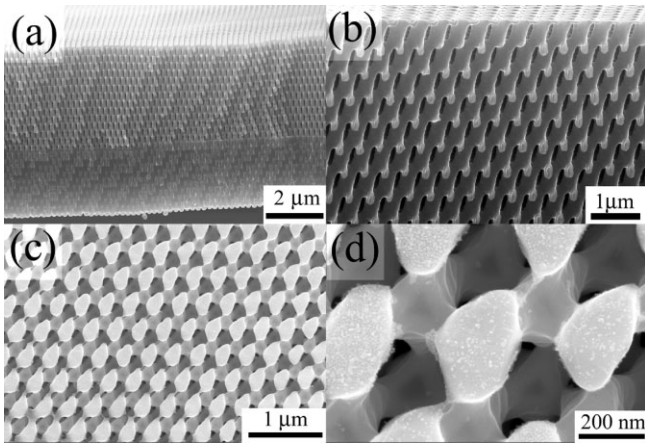
Figure 2. Inverted TiO$_2$ photonic crystal formed after template removal by O$_2$ plasma etch. a,b) Cross sections revealed by cleavage along a (11$\bar{1}$) plane. c,d) Top (111) surface of film.

Figure 3. Microreflectivity (R) and microtransmission (T) for a) a holographically defined polymer template; b) a template infiltrated with TiO$_2$; c) a TiO$_2$ photonic crystal after the template had been removed. In all cases, the shaded bands indicate the calculated position and width of the fundamental and second order (111) photonic bandgaps.

transmission at normal incidence from the same location on the sample (spot diameter 200 μm). Figure 3a shows reflectivity and transmission spectra of the polymer/air template. A peak in the reflectivity and a corresponding dip in transmission were observed at ~1485 and 1430 nm, respectively, close to the calculated position of the fundamental (111) stop band; a strong reflectivity peak and transmission dip at 790 nm correspond to the second-order stop band (calculated stop bands for an infinite photonic crystal are indicated by shading). Infiltration with TiO$_2$ to produce a polymer/TiO$_2$/air composite increases the average refractive index and decreases the index contrast of the photonic-crystal film, resulting in a red shift of all gaps and a narrowing of the fundamental gap (Fig. 3b). The reflectivity peak and transmission dip corresponding to the fundamental gap were both observed at ~1935 nm, consistent with the calculated band structure; both features were narrower by a factor of ~2 than in the case of the polymer/air template. The second-order stop band was observed at 1000 nm. Figure 3c shows the optical properties of the final TiO$_2$ photonic crystal. As expected, removal of the polymer template shifted the stop bands back to shorter wavelengths (1600 and 828 nm), in excellent agreement with band-structure calculations. The reflectivity peak and transmission dip both widened, although remained significantly narrower than in the case of the polymer/air template.

Evidence for the optical quality of the inverted photonic crystal is provided by the increase in peak reflectivity from 20 % for the template to 65 % for the TiO$_2$/air structure and by the consistent agreement between observed stop-band positions and the predictions of band-structure calculations. Finite-thickness broadening of both transmission dips and reflectivity peaks by at least ~100 nm in all three cases is expected.[30] Additional broadening is caused by structural variations[31] caused by the attenuation of the holographic exposure by ~10 % through the thickness of the film. (We have shown, by synthesizing related dendrimeric epoxide based resists, that the extrinsic absorption that dominates the absorption of resists based on commercial SU-8 can be substantially reduced.) We expect fabrication by conformal deposition to reduce the effect of both random and systematic variations of the filling factor of the template, as the filling fraction of the conformally deposited shell varies more slowly than that of the template itself. We estimate that the systematic depth-dependent change in filling factor caused by resist absorption broadens stop-band features by 50 nm for the polymer template but only 20 nm for the TiO$_2$ replica, consistent with the observed narrowing of stop-band features in the spectra of the TiO$_2$/air photonic crystal. A reduction in disorder in the TiO$_2$ replica relative to the polymer template is
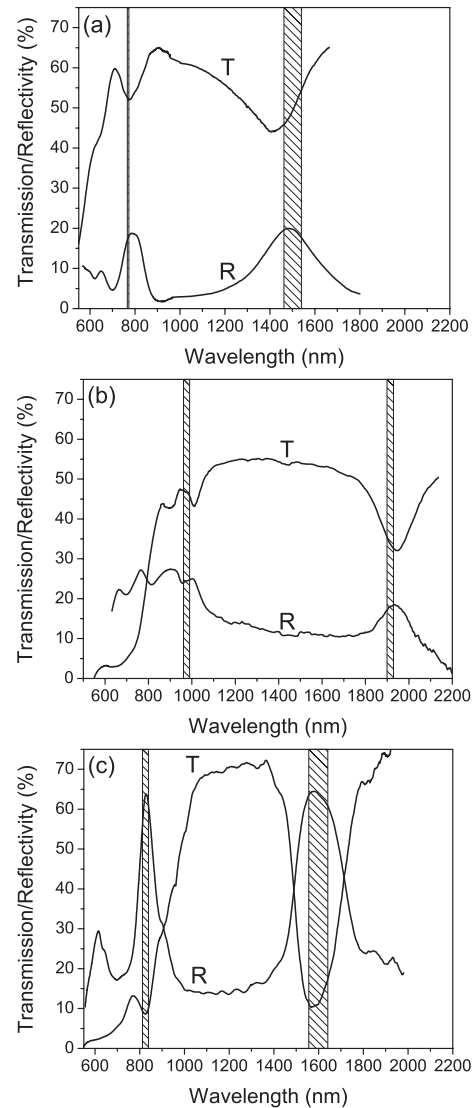
consistent with the observed steepening of the edges of the stop-band features in the spectra of the TiO$_2$/air photonic crystal.[32]

In summary, we have demonstrated that the combination of holographic lithography and atomic layer deposition allows rapid and flexible fabrication of 3D photonic crystals. A high-quality photonic crystal in amorphous TiO$_2$ was produced by conformal infiltration followed by etching of a holographically defined polymeric template. To our knowledge, this is the first demonstration of the production and optical characterization of a high-quality, high-index 3D photonic crystal using holographic lithography. Reflectivity and transmission measurements are consistent with predicted photonic-band-gap positions. The spectra provide no evidence for structural degradation during processing; changes in reflectivity peaks and transmission minima are consistent with an *increase* in optical uniformity associated with conformal growth. The fabrication process demonstrated here can be combined with two-photon writing of embedded device structures[2] to create an integrated technique for the production of all-optical circuits,[1] microcavity-based light emitters,[33] and other micro-structured photonic devices.[34]

Experimental

Photoresist was prepared from SU-8 resin (Resolution Performance Products) (58 wt %) dissolved in cyclopentanone (39 wt %) with 3 wt % triarylsulfonium hexafluoroantimonate photoacid generator solution (50 wt % in propylene carbonate). Fused silica substrates were spin-coated with approximately 10 μm of resist; solvent was removed by baking (5 min at 55 °C, 10 min at 95 °C then 2.5 min at 55 °C). Holographic exposure by an interference pattern with *R*32 symmetry, described in a previous publication [29], was carried out using a single 6 ns pulse from a frequency-tripled, injection-seeded Nd:yttrium aluminum garnet (YAG) laser (Spectra Physics) with an average energy density of 25 mJ cm^{-2}. After exposure, the resist was developed by baking at 55 °C for 1 h, washing in propylene glycol monomethyl ether acetate, rinsing in isopropyl alcohol, and drying in air.

The ALD reactor was comprised of a Thermolyne tube furnace with a single zone that houses the sample-deposition area, an Alcatel roughing pump and chemical scrubber system, a precursor delivery system, and a nitrogen purge. The precursor gases, derived from the vapor pressure of room-temperature-liquid sources, were introduced to a N$_2$ carrier gas using computer-controlled solenoid valves. Nitrogen flow for each precursor was regulated using mass-flow controllers. TiO$_2$ was grown within the template using alternating 8 s pulses of TiCl$_4$ (Alfa Aesar) and H$_2$O, each separated by a 20 s, 225 sccm N$_2$ purge, while maintaining the substrate at 100 °C. The vacuum level within the reactor was ~500 mTorr during pulses, and 200 mTorr during purges.

The surface of the infiltrated template was ion-milled with a 0.5 mA, 4 keV Ar$^+$ beam (Gatan) at 15° incidence for 15 min. Plasma etching was accomplished using a barrel etcher (LFE) operated for 1 h at 300 W.

Removal of the crosslinked polymer template by pyrolysis was also tried and found to be unsatisfactory: temperatures in excess of 400 °C were required, and thermal stresses caused considerable damage to the photonic crystal.

All SEM images were acquired using a LEO 1530 scanning electron microscope.

Reflectivity and transmission spectra were acquired using a custom microreflectivity/microtransmission system. A 10× objective with a numerical aperture of 0.25 was used with field and condenser diaphragms closed, minimizing divergence (measured to be < 8°) and reducing the spot size to 200 μm. A spectral range of 550–2200 nm was explored using a tungsten–halogen lamp and a combination of silicon (Thorlabs), indium gallium arsenide (Thorlabs), and lead sulfide (Electro-optical Systems, Inc) detectors; an optical chopper (Edmund Optics) and lock-in amplifier (Princeton Applied Research) were used for signal acquisition.

The boundary between high- and low-dielectric-constant material in a holographically defined photonic crystal corresponds approximately to a surface of constant intensity in the original interference pattern, determined by the threshold exposure above which the resist is rendered insoluble. For the purpose of defining the distribution of dielectric for photonic-band-structure calculations, a threshold intensity surface was chosen to match the polymer-filling fraction of 46 % deduced from SEM images of TiO$_2$ replicas. This surface was scaled uniformly in linear dimensions by 0.85 to account for shrinkage during development and to match the observed lattice spacing. The distribution of TiO$_2$ in the infiltrated structures, before and after removal of the template, was approximated by assuming conformal deposition of a 50 nm layer on the polymer surface, corresponding to a TiO$_2$ filling fraction of ~30 %. Refractive indices of 1.6 and 2.3 for SU-8 resist and ALD-deposited TiO$_2$, respectively, were used. Photonic band structures were calculated using the MIT Photonic Bands Package [35].

[1] M. Soljacic, J. D. Joannopoulos, *Nat. Mater.* **2004**, *3*, 211.

[2] J. Scrimgeour, D. N. Sharp, C. F. Blanford, O. M. Roche, R. G. Denning, A. J. Turberfield, *Adv. Mater.* **2006**, *18*, 1557.

[3] M. Campbell, D. N. Sharp, M. T. Harrison, R. G. Denning, A. J. Turberfield, *Nature* **2000**, *404*, 53.

[4] B. H. Cumpston, S. P. Ananthavel, S. Barlow, D. L. Dyer, J. E. Ehrlich, L. L. Erskine, A. A. Heikal, S. M. Kuebler, I.-Y. S. Lee, D. McCord-Maughon, J. Qin, H. Röckel, M. Rumi, X.-L. Wu, S. R. Marder, J. W. Perry, *Nature* **1999**, *398*, 51.

[5] H.-B. Sun, S. Matsuo, H. Misawa, *Appl. Phys. Lett.* **1999**, *74*, 786.

[6] M. Deubel, G. von Freymann, M. Wegener, S. Pereira, K. Busch, C. M. Soukoulis, *Nat. Mater.* **2004**, *3*, 444.

[7] S. Kawata, H.-B. Sun, T. Tanaka, K. Takada, *Nature* **2001**, *412*, 697.

[8] H.-B. Sun, A. Nakamura, K. Kaneko, S. Shoji, S. Kawata, *Opt. Lett.* **2005**, *30*, 881.

[9] E. Yablonovitch, T. J. Gmitter, R. D. Meade, A. M. Rappe, K. D. Brommer, J. D. Joannopoulos, *Phys. Rev. Lett.* **1991**, *67*, 3380.

[10] C. T. Chan, K. M. Ho, C. M. Soukoulis, *Europhys. Lett.* **1991**, *16*, 563.

[11] M. Maldovan, A. M. Urbas, N. Yufa, W. C. Carter, E. L. Thomas, *Phys. Rev. B: Condens. Matter Mater. Phys.* **2002**, *65*, 165 123.

[12] D. N. Sharp, A. J. Turberfield, R. G. Denning, *Phys. Rev. B: Condens. Matter Mater. Phys.* **2003**, *68*, 205 102.

[13] Y. A. Vlasov, X.-Z. Bo, J. C. Sturm, D. J. Norris, *Nature* **2001**, *414*, 289.

[14] A. Blanco, E. Chomski, S. Grabtchak, M. Ibisate, S. John, S. W. Leonard, C. López, F. Meseguer, H. Míguez, J. P. Mondia, G. A. Ozin, O. Toader, H. M. van Driel, *Nature* **2000**, *405*, 437.

[15] H. Míguez, N. Tétreault, B. Hatton, S. M. Yang, D. Perovic, G. A. Ozin, *Chem. Commun.* **2002**, 2736.

[16] H. Míguez, N. Tétreault, S. M. Yang, V. Kitaev, G. A. Ozin, *Adv. Mater.* **2003**, *15*, 597.

[17] a) J. E. G. J. Wijnhoven, W. L. Vos, *Science* **1998**, *281*, 802. b) J. E. G. J. Wijnhoven, L. Bechger, W. L. Vos, *Chem. Mater.* **2001**, *13*, 4486.

[18] G. Subramanian, V. N. Manoharan, J. D. Thorne, D. J. Pine, *Adv. Mater.* **1999**, *11*, 1261.

[19] a) M. Ritala, M. Leskelä, in *Handbook of Thin Film Materials*, Vol. I (Ed: H. S. Nalwa), Harcourt Academic, London, UK **2002**, Ch. 2. b) M. Ritala, *Appl. Surf. Sci.* **1997**, *112*, 223.

[20] J. S. King, E. Graugnard, C. J. Summers, *Adv. Mater.* **2005**, *17*, 1010.

[21] J. S. King, D. Heineman, E. Graugnard, C. J. Summers, *Appl. Surf. Sci.* **2005**, *244*, 511.

[22] A. Rugge, J. S. Becker, R. G. Gordon, S. H. Tolbert, *Nano Lett.* **2003**, *3*, 1293.

[23] J. S. King, C. W. Neff, C. J. Summers, W. Park, S. Blomquist, E. Forsythe, D. Morton, *Appl. Phys. Lett.* **2003**, *83*, 2566.

[24] M. Scharrer, X. Wu, A. Yamilov, H. Cao, R. P. H. Chang, *Appl. Phys. Lett.* **2005**, *86*, 151 113.

[25] R. G. Gordon, D. Hausmann, E. Kim, J. Shepard, *Chem. Vap. Deposition* **2003**, *9*, 73.

[26] a) J. Aarik, A. Aidla, T. Uustare, V. Sammelselg, *J. Cryst. Growth* **1995**, *148*, 268. b) M. Ritala, M. Leskela, E. Nykanen, P. Soininen, L. Niinisto, *Thin Solid Films* **1993**, *225*, 288.

[27] J. D. Ferguson, A. W. Weimer, S. M. George, *Chem. Mater.* **2004**, *16*, 5602.

[28] D. Heineman, *M. S. Thesis*, Georgia Institute of Technology **2004** (http://etd.gatech.edu/theses/available/etd-05142004-143254/).

[29] E. R. Dedman, D. N. Sharp, A. J. Turberfield, C. F. Blanford, R. G. Denning, unpublished.

[30] J. F. Bertone, P. Jiang, K. S. Hwang, D. M. Mittleman, V. L. Colvin, *Phys. Rev. Lett.* **1999**, *83*, 300.

[31] R. C. Rumpf, E. G. Johnson, *J. Opt. Soc. Am. A* **2004**, *21*, 1703.

[32] M. S. Thijssen, R. Sprik, J. E. G. J. Wijnhoven, M. Megens, T. Narayanan, A. Lagendijk, W. L. Vos, *Phys. Rev. Lett.* **1999**, *83*, 2730.

[33] C. Weisbuch, H. Benisty, *Solid State Commun.* **2005**, *135*, 627.

[34] *Roadmap on Photonic Crystals* (Eds: S. Noda, T. Baba), Springer, Berlin, Germany **2003**.

[35] S. G. Johnson, J. D. Joannopoulos, *Opt. Express* **2001**, *8*, 173.

_____